

Refined position angle measurements for galaxies of the SDSS Stripe 82 co-added dataset

József Varga^{1,*}, István Csabai¹ and László Dobos¹

July 12, 2018

Key words galaxies: fundamental parameters – methods: data analysis – techniques: image processing – catalogs – cosmology: large-scale structure

Abstract

Position angle measurements of Sloan Digital Sky Survey (SDSS) galaxies, as measured by the surface brightness profile fitting code of the SDSS photometric pipeline (Lupton et al. 2001), are known to be strongly biased, especially in the case of almost face-on and highly inclined galaxies. To address this issue we developed a reliable algorithm which determines position angles by means of isophote fitting. In this paper we present our algorithm and a catalogue of position angles for 26397 SDSS galaxies taken from the deep co-added Stripe 82 (equatorial stripe) images. Data are published online at <http://www.vo.elte.hu/galmorph>.

1 Introduction

Reliable shape and position angle measurements of galaxies are essential for a number of fields of extragalactic astronomy including the investigation of correlations between the orientation and spatial distribution of galaxies, weak lensing, etc. Shape measurement algorithms, however, are known to be subject to various unwanted effects (e.g. Byun & Freeman 1995). Assuming that the pixels of a galaxy are distributed elliptically – which is a rather simple yet suitable approximation in most cases – two primary parameters are to be obtained: the axis ratio b/a and the position angle ϕ , measured with respect to the north direction. In case of disc galaxies, the axis ratio can be easily transformed into the inclination angle (i), hence the direction of the rotation axis can be obtained. There remains an ambiguity in the sign of the rotation axis, however, because the “approaching” and “receding” sides of the disc are hard to be distinguished based on optical images. Spectroscopic and HI measurements, which would yield the required information, are not yet feasible at the scale of optical surveys. In case of elliptical galaxies, even if they are rotationally supported, the determination of the directions of axes depends

even more on the projection effects.

1.1 Position angle measurements in the SDSS

The Sloan Digital Sky Survey (York et al. 2000) is the largest wide-field photographic survey to date with more than 400 million catalogued objects. The SDSS catalogue provides extensive information on the morphology of the sources. Ellipticities and position angles are measured using four different methods:

- The first method is based on surface brightness profile fits. Two models are fitted to the two-dimensional images of each object: a pure exponential and a pure de Vaucouleurs’ profile. The model fits give estimates on the axis ratio $(b/a)_{\text{exp}}$ and $(b/a)_{\text{dev}}$, and the position angle ϕ_{exp} and ϕ_{dev} . These fits also take the PSF into account.
- The second method is based on flux-weighted second moments, referred as “Stokes parameters” in the catalogue (denoted with Q and U). Stokes parameters can be used to reconstruct the axis ratio and the position angle. The performance of these parameters, however, is not ideal at low signal-to-noise ratio. (Stoughton et al. 2002)
- The third method is based on adaptive moments (Bernstein & Jarvis 2002) which are the second moments of the object intensity measured using a radial weight function iteratively adapted to the shape (ellipticity) and size of the object. This is well suited for cosmic shear measurements, however, contrary to the second method, it is not model independent. (Bartelmann et al. 2012)
- The last method determines the ellipticity of the 25 mag arcsec⁻² isophote by measuring the radius of the isophote as a function of angle $r(\phi)$. The major and minor axes (a_{iso} , b_{iso}) and the position angle (ϕ_{iso}) are then extracted from the coefficients of the Fourier expansion of $r(\phi)$. Isophotal quantities turned out to be unreliable and have been dropped from the catalogue since Data Release 8 (Aihara et al. 2011).

Note that the last three methods do not account for the varying seeing. For more details on SDSS image processing algorithm, refer to Stoughton et al. (2002).

*E-mail: jozsef-varga@caesar.elte.hu

¹Department of Physics of Complex Systems, Eötvös Loránd University, Pf. 32, H-1518 Budapest, Hungary

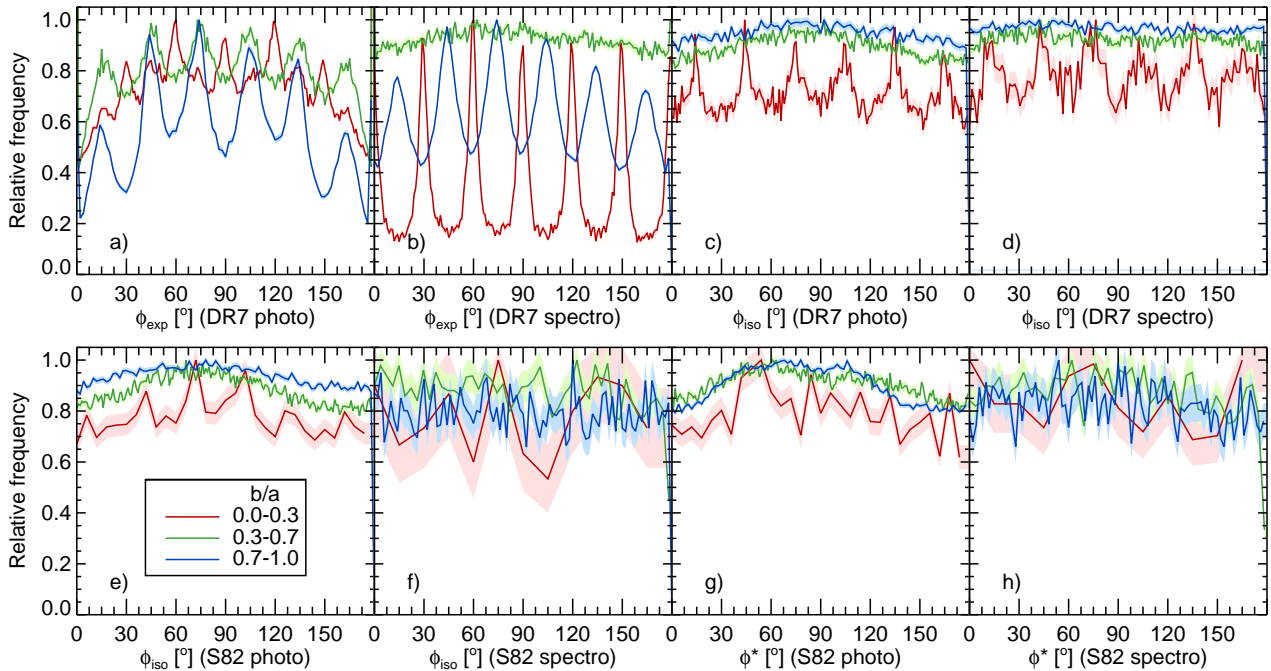


Figure 1: Distribution of position angles (r band, respect to the longer image side) of SDSS galaxies. Each panel shows the distribution of the sample divided into three axial ratio bins. Data were collected from the full DR7 catalogue (upper panels), and from the Stripe 82 co-added catalogue (panels e and f). Data in panels g and h are from the current analysis.

Table 1: Statistics of the source list (number of processed objects and the chosen magnitude limits), and the percentage of the fitted and rejected objects in each photometric filter.

Filter	Source list statistics		Fit statistics	
	Number	Mag. limit	Rejected (%)	Fitted (%)
u	80472	20	53.6	46.4
g	1114774	22	33.9	66.1
r	2645180	22	53.9	46.1
i	1956496	21	41.1	58.9
z	1079363	20	52.9	47.1

1.2 Biased distribution of SDSS position angles

In Fig. 1 we plot the histogram of position angles from the exponential model fits ϕ_{exp} (panels a and b), from the isophotal methods ϕ_{iso} (panels c through f), and from the present analysis ϕ^* (panels g and h) for the entire (morphologically identified) galaxy sample (panels a, c, e and g) and only for the spectroscopically confirmed main galaxy sample (panels b, d, f and h) (Strauss et al. 2002). The colours refer to three different axis ratio intervals, see figure caption. It is obvious from Fig. 1 that the distribution of ϕ_{exp} , as measured by the SDSS pipeline, is heavily biased by systematic effects. A huge periodic modulation can be clearly seen in the relative frequency of ϕ_{exp} with a period of 30° in the $b/a = 0.0-0.3$ and (with opposite phase) in the $b/a = 0.7-1.0$ subsamples (panels a and b). Significant differences between the entire photo sample and the

spectro sample are also apparent. While the bias of ϕ_{exp} is even stronger for edge-on and face-on galaxies in the spectro sample, it disappears for the intermediate $b/a = 0.3-0.7$ subsample. Interestingly, ϕ_{iso} shows similar bias, but only in the case of highly inclined galaxies (red line in panels c and d). We mention that a very similar systematic distortion of b/a is also observable, with a period of 0.1 (see Fig. 2). Distributions are plotted for SDSS DR7 but the bias is still present in DR8 and DR9.

1.3 Origin of the strong systematic bias

To our best understanding the strong bias in the distribution of ϕ_{exp} is caused by the surface brightness fitting algorithm of the SDSS photo pipeline. As fitting a three parameter ($r_e, a/b, \phi_{\text{exp}}$) profile to two dimensional images is computationally expensive, the photo pipeline uses precomputed tables of models. To use these tables, first radial profiles have to be binned into 30° sectors of annuli around the object centroids which introduces a preference of multiples of 30° in ϕ_{exp} . Apparently, the χ^2 -minimization algorithm fails to move away from the local minima of the precomputed models by varying ϕ and the 30° binning propagates into the final fits. The situation is even more severe in case of spectroscopically confirmed galaxies.

2 Improved isophote fitting algorithm

Because the available position angle data of SDSS galaxies are unreliable we decided to develop our own isophote

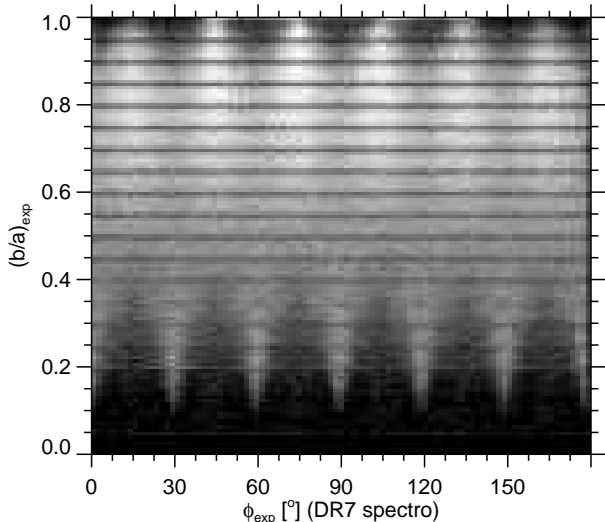


Figure 2: Two dimensional histogram of r -band position angles (respect to the longer image side) and axis ratios of galaxies from the spectroscopically confirmed main galaxy sample (same data as in Fig. 1 panel b). The square root of the frequency counts is scaled to 8-bit greyscale pixels.

fitting algorithm and software tools written in IDL¹. The algorithm automatically identifies the most reliable isophote surface brightness for each frame, determines this isophote of each object and fits an ellipse to it. The main steps of image processing are as follows.

- Read in a calibrated image.
- Choose a global surface brightness level to find the most reliable isophotes. Here we fit a Gaussian to the histogram of pixel values of the whole frame, from which we get the mean background level and the noise σ . The 4σ level is chosen as the surface brightness of the isophotes.
- Detect the isophotes with the CONTOUR routine of the standard IDL library. Isophotes are returned as contour polygons given in pixel coordinates.
- Match the objects from the source list with contour polygons. Here we use a matching radius of $3.6''$ (9 px).
- Check the “quality” of the contours and reject those that are too small to fit reliably, i.e. having less than 10 edges.
- Fit ellipses to the contours. Fitting is performed using the MPFIT routine. MPFIT is a port to IDL of the non-linear least squares fitting program MINPACK-1 (Markwardt 2009) and, thus is not part of the standard IDL library. The routine returns five parameters: the X and Y coordinates of the centroid, length of the minor and major axis, and the position angle with respect to the pixel coordinate system.

¹The code is available from the authors on request.

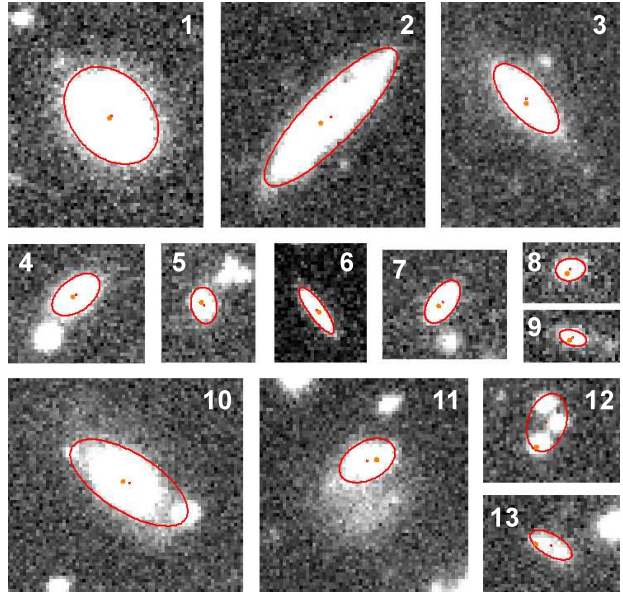


Figure 3: Examples of galaxies overplotted with the ellipses fitted to the 4σ isophotes by our algorithm. Images 1–9 are good fits, while images 10–13 are not. The galaxy in image 11 has complex morphology, hence our elliptical model is not appropriate. In image 10, 12 and 13 there is an other source so close to the object in question, that the isophotes are blended, biasing the elliptical fit.

In Fig. 3 we show several images of galaxies overplotted with the fitted ellipses. See caption for detailed description.

Fits are automatically rejected if the contours do not match unambiguously a single object or because the contour polygons are too small. A small fraction of the objects is fitted incorrectly due to blended isophotes. The centroids of the fitted ellipses in these cases are a few pixels off the source positions as measured by the SDSS photo pipeline. The percentage of rejected and successfully fitted objects is listed in Tab 1. Depending on the imaging filter a 46–66% of the objects are fitted successfully.

In Fig. 4 we compare our position angles ϕ^* to those by SDSS (ϕ_{exp} and ϕ_{iso}). The correlation of our position angle estimates with ϕ_{exp} is stronger than with ϕ_{iso} , which is interesting as our method is essentially an isophote fitting method. The imprints of the strong bias in ϕ_{exp} are visible as horizontal stripes in the middle and right panes.

A drawback of our isophote fitting algorithm is that it does not account for seeing. As we do not deconvolve the PSF from the input images, smaller objects seem to be more circular. This is not expected to affect our final catalogue significantly because the median radius of our sample is $6''$ in the r -band, much larger than the typical SDSS PSF of $1.4''$ FWHM.

3 Data and sample selection

We base our new catalogue of improved position angle measurements on u , g , r , i and z -band calibrated images taken from the SDSS Stripe 82 data set (Abazajian et al. 2009). The Stripe 82 images were co-added from about 20–40

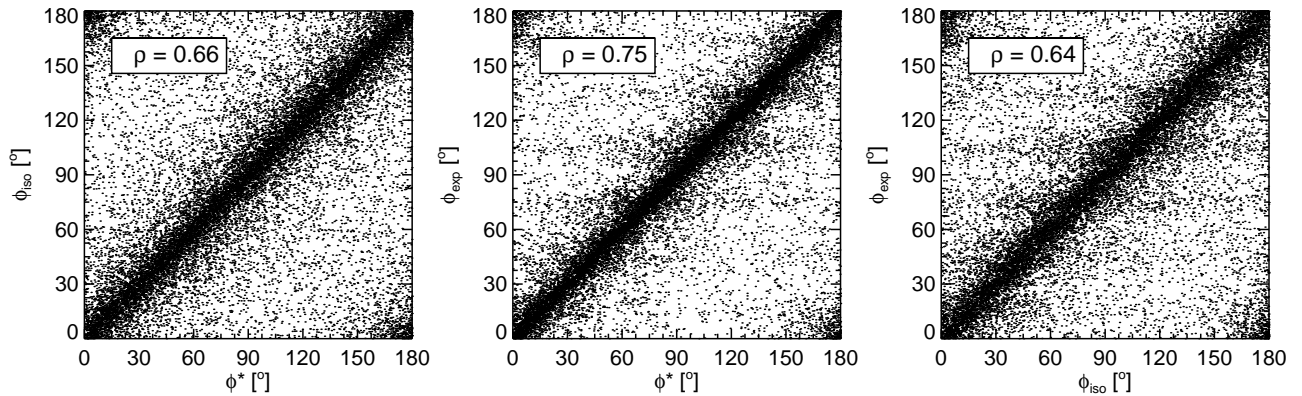


Figure 4: Comparison plots of position angles determined by our algorithm (ϕ^*) and those by the SDSS photo pipeline (ϕ_{exp} and ϕ_{iso}) for the r -band Stripe 82 co-added images. Over 20,000 points are plotted in each diagram. The corresponding correlation coefficients ρ are also denoted.

individual exposures and the reduced catalogue has got an estimated r -band magnitude limit of about $r \lesssim 24$ mag, which is about one magnitude deeper than the rest of SDSS (Gunn et al. 1998). The survey footprint is a 2.5° wide stripe along the celestial equator ($-50^\circ \leq \alpha \leq 59^\circ$, $|\delta| \leq 1.26^\circ$).

The reason behind choosing the Stripe 82 data despite its limited footprint was that these co-added images provide far better signal-to-noise ratio than the single-exposure SDSS images, thus we can expect more reliable isophote fits.

We select objects from the co-added catalogue that are morphologically classified as galaxies and are brighter than a given magnitude in each band. Tab. 1 lists the chosen magnitude limits for each photometric filter and the number of sources selected. Our algorithm outlined in Sec. 2 relies on precise source positions as input parameters; we take these positions from the Stripe 82 catalogue.

4 Our unbiased catalogue

Our image processing software outputs the fitted parameters with uncertainties and various other control parameters. To compile a catalogue from our data, we make use of the existing photometric and spectroscopic information from the SDSS Stripe 82 co-added survey. The catalogue contains the object identifiers, celestial coordinates, model magnitudes in each band, redshift, velocity dispersion, *eClass* from the SDSS co-added catalogue, and, of course, the morphological parameters given by this work. These are the major axis, minor axis, the X and Y coordinates of the centroids and the position angle of the fitted ellipse in each photometric filter. Please note, that errors of the morphological parameters are likely to be overestimated, especially in case of the position angle, by the MPFIT routine. We include additional parameters: the number of edges of the contour polygons, the maximal intensity in a 3 by 3 pixel region around the ellipse centroids and around the original source coordinates.

The catalogue is available on-line at <http://www.vo.elte.hu/galmorph>.

5 Discussion and future work

The extreme bias identified in the position angle measurements of SDSS galaxies has strong implications in many fields of interest and might spoil important results. For instance, correlations between the orientation and spatial distribution of galaxies have long been studied but only the deep, large-scale optical surveys of the last decade made more elaborate investigation of this topic possible. Thus, it is extremely important to make sure these large catalogues contain reliable data. We are currently working on a more detailed statistical analysis of our algorithm that will be published in the near future.

Acknowledgements. This work was supported by the following Hungarian grants: NKTH: Polányi, KCKHA005 and OTKA-103244.

References

- Abazajian, K. N., et al. 2009, *ApJS*, 182, 543
- Aihara, H., Allende Prieto, C., An, D., et al. 2011, *ApJS*, 193, 29
- Bartelmann, M., Viola, M., Melchior, P., & Schäfer, B. M. 2012, *A&A*, 547, A98
- Bernstein, G. M., & Jarvis, M. 2002, *AJ*, 123, 583
- Byun, Y. I., & Freeman, K. C. 1995, *ApJ*, 448, 563
- Gunn, J. E., Carr, M., Rockosi, C., et al. 1998, *AJ*, 116, 3040
- Lupton, R., Gunn, J. E., Ivezić, Z., et al. 2001, *Astronomical Data Analysis Software and Systems X*, 238, 269
- Markwardt, C. B. 2009, *Astronomical Data Analysis Software and Systems XVIII*, 411, 251
- Stoughton, C., Lupton, R. H., Bernardi, M., et al. 2002, *AJ*, 123, 485
- Strauss, M. A., Weinberg, D. H., Lupton, R. H., et al. 2002, *AJ*, 124, 1810
- York, D. G., Adelman, J., Anderson, J. E., Jr., et al. 2000, *AJ*, 120, 1579